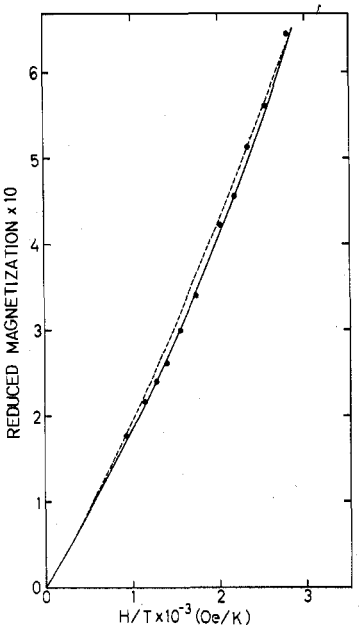

Figure 3. Comparison of the present calculation of the magnetic moment with the experimental data of Jeter et al. shown by solid circles. The results giving the best fit by the cluster model and by the modified effective field model are shown by the dotted and solid lines, respectively.

model in which the intra- and interchain exchange interactions are equally taken into consideration.

Let us consider a cluster of four spins $\mathbf{s}_1$, $\mathbf{s}_2$, $\mathbf{s}_3$, and $\mathbf{s}_4$ as shown in Figure 1 and take into account the intrachain exchange interaction between spins $\mathbf{s}_1$ ($\mathbf{s}_2$) and $\mathbf{s}_3$ ($\mathbf{s}_4$) and the interchain exchange between spins $\mathbf{s}_1$ and $\mathbf{s}_2$. Other spin–spin interactions operating through the bridging carbonate groups (i.e., along the chains) will be considered as an effective molecular field afterward. The spin Hamiltonian of the Heisenberg exchange interactions in the present four-spin cluster under an external magnetic field is given by

$$\mathcal{H} = -2J(\mathbf{s}_1\cdot\mathbf{s}_2) - 2J'[(\mathbf{s}_1\cdot\mathbf{s}_3) + (\mathbf{s}_2\cdot\mathbf{s}_4)] + g\mu_B H\sum_{i=1}^{4} s^z{}_i \quad (1)$$

Here, we have neglected the antisymmetric exchange interactions[5] which may coexist with the intrachain exchange interactions.

The conventional vector-model approach to the cluster spin system cannot be applied for the present spin Hamiltonian (eq 1), because the composite spins $\mathbf{S} = \mathbf{s}_1 + \mathbf{s}_2$, $\sigma_1 = \mathbf{s}_1 + \mathbf{s}_3$, and $\sigma_2 = \mathbf{s}_2 + \mathbf{s}_4$ are not diagonalized simultaneously. For convenience, we choose the basis wave functions which diagonalize the second term of eq 1. Then the 16 × 16 secular matrix for the Hamiltonian (eq 1) breaks up into two 1 × 1, two 4 × 4, and one 6 × 6 submatrices.

With the use of spin wave functions $\psi(s_i)$ which are either α or β when $s^z{}_i = +^1/_2$ or $-^1/_2$, respectively, the basis wave functions $\psi(s_1)\,\psi(s_3)\,\psi(s_2)\,\psi(s_4)$ for each submatrix are given as follows:

$$\left.\begin{matrix}\alpha\alpha\alpha\alpha\\ \beta\beta\beta\beta\end{matrix}\right\}(m=\pm 2)$$

$$\left.\begin{matrix}(\alpha\alpha\alpha\beta \pm \alpha\alpha\beta\alpha)/2^{1/2}\\ (\alpha\beta\alpha\alpha \pm \beta\alpha\alpha\alpha)/2^{1/2}\end{matrix}\right\}(m=1)$$

$$\left.\begin{matrix}(\beta\beta\alpha\beta \pm \beta\beta\beta\alpha)/2^{1/2}\\ (\alpha\beta\beta\beta \pm \beta\alpha\beta\beta)/2^{1/2}\end{matrix}\right\}(m=-1) \quad (2)$$

$$\left.\begin{matrix}\alpha\alpha\beta\beta\\ \beta\beta\alpha\alpha\\ (\alpha\beta\alpha\beta \pm \alpha\beta\beta\alpha + \beta\alpha\alpha\beta \pm \beta\alpha\beta\alpha)/2\\ (\alpha\beta\alpha\beta \pm \alpha\beta\beta\alpha - \beta\alpha\alpha\beta \mp \beta\alpha\beta\alpha)/2\end{matrix}\right\}(m=0)$$

m is the z component of the total composite spin and has the definite diagonal elements in each submatrix. The eigenvalues of each secular submatrix are obtained as a function of exchange parameters J and J' and the magnetic field H.

With the eigenvalues $\epsilon_{m,i}$, the magnetic moment can be calculated by

$$M = Ng\mu_B\sum_{m,i} m\exp(-\epsilon_{m,i}/kT)/\sum_{m,i}\exp(-\epsilon_{m,i}/kT) \quad (3)$$

For comparison with the experimental data, the numerical calculation has been done for $g = 2.18$, for the field strengths of 10.0, 12.5, and 15.0 kOe, and for various sets of values of J and J'. The calculation has been performed by the FACOM M-190 computing facility of Kyushu University. The reduced magnetic moment $\langle\mu\rangle = M/(N\mu_B/2)$ as a function of H/T should be compared with the experimental data by Jeter et al. The variation of $\langle\mu\rangle = f(H/T)$ for various sets of values of J and J' are shown in Figure 2. The fitting procedure, in consideration of these data, has resulted in the values $J = +2.34$ cm^{-1} and $J' = +2.52$ cm^{-1} which are both ferromagnetic contrary to the estimates of Jeter et al. As shown in Figure 3, the calculation of the magnetic moment with this set of values gives far better agreement with the experimental magnetic moment than those of the dimer model.

The intrachain exchange interactions other than those considered in the present cluster model result in an effective molecular field. Then the reduced magnetic moment may be modified in the first approximation as

$$\langle\mu\rangle = f(H/T)/(1 - \Theta/T) \quad (4)$$

The fitting procedure with the use of this modified expression gives a quite excellent agreement with the variation of the experimental magnetic moment as shown in Figure 3. The values of the parameters in this case have been estimated as $J = -2.0$ cm^{-1}, $J' = +1.0$ cm,$^{-1}$ and $\Theta = 1.5$ K. For negative values of J' the fitting procedures were unsuccessful, as in the case of the linear-chain model by Jeter et al. In view of the copper–carbonate–copper angle (119°), the ferromagnetic intrachain exchange coupling may be reasonable.[6] These values are also quite reasonable for the interpretation of the behavior of the magnetic susceptibility which is antiferromagnetic in nature. Thus, the present exchange model of a four-spin cluster provides a much improved analysis of magnetic interactions for diamminecopper(II) carbonate, and so may be a more realistic model than the antiferromagnetic linear-chain model or the dimer model previously proposed by Jeter et al.

Registry No. $Cu(NH_3)_2CO_3$, 21710-50-9.

References and Notes

(1) Y. Jeter, D. J. Hodgson, and W. E. Hatfield, *Inorg. Chem.*, **11**, 185 (1972).
(2) F. Hanic, *Acta Chim. Acad. Sci. Hung.*, **32**, 305 (1962).
(3) F. Hanic, *Chem. Zvesti*, **17**, 365 (1963).
(4) M. Inoue, M. Kishita, and M. Kubo, *Inorg. Chem.*, **6**, 900 (1967).
(5) T. Moriya, *Phys. Rev.*, **120**, 91 (1960).
(6) J. Kanamori, *J. Phys. Chem. Solids*, **10**, 87 (1959).

Contribution from the Department of Chemistry, University of Vermont, Burlington, Vermont 05401

Physical and Chemical Properties of Squarate Complexes. 1. Spectral, Magnetic, and Thermal Behavior of Dimeric Iron(III) Squarate

James T. Wrobleski and David B. Brown*

Received December 22, 1977

Trivalent metal–ion complexes which contain the squarate dianion (I, Sq) with general formula $M(Sq)(OH)(H_2O)_3$ were

0020-1669/78/1317-2959$01.00/0

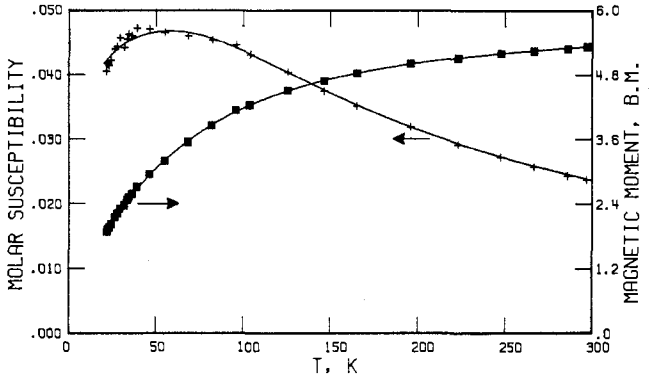

Figure 1. Effective magnetic moment for $[Fe(Sq)(OH)(H_2O)_2]_2 \cdot 2H_2O$. The solid line gives the theoretical moment obtained for an exchange-coupled $S_1 = S_2 = {}^5/_2$ dimer with $J = -6.9$ cm^{-1} and $g = 2.00$.

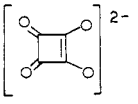

I

first reported by West and Niu[1] (M = Al, Cr, or Fe) and Condren and McDonald[2] (M = V). Niu's suggestion of a dimeric structure for $Fe(Sq)(OH)(H_2O)_3$ was principally supported by the reduced room-temperature magnetic moment of this compound. The other trivalent metal complexes were subsequently assigned dimeric structures based on their X-ray isomorphism to the iron compound.[1,2]

As part of our investigation of the electronic and structural properties of metal-squarate complexes we have studied the variable-temperature magnetic susceptibility and spectral and thermal behavior of $Fe(Sq)(OH)(H_2O)_3$ and report here evidence which supports a dihydroxy-bridged dimeric structure (II) for this complex.

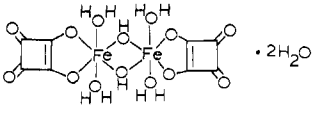

II

Experimental Section

Materials and Methods. Squaric acid (3,4-dihydroxy-3-cyclobutene-1,2-dione) was purchased from Aldrich Chemical Co. and used as received. $FeCl_3 \cdot 6H_2O$ was purified by centrifuging a concentrated ethanolic solution of commercial hydrated ferric chloride and discarding the insoluble material. Magnetic susceptibilities were determined using a conventional Faraday balance calibrated with $Hg[Co(NCS)_4]$.[4] Ligand diamagnetism was treated as usual by assuming $\chi_{sq} = -30.6 \times 10^{-6}$ cgsu and by using a table of Pascal's constants.[5] Mössbauer spectra were obtained by using the spectrometer previously described[6] with a $^{57}Co(Pt)$ source maintained at room temperature. A moderately thin foil of natural α-Fe was used to define the velocity scale. Mössbauer spectra were deconvoluted by assuming pure Lorentzian line shapes superimposed on a parabolic baseline. Parameters obtained in this manner were reproducible to ±1%. Infrared spectra were obtained on a Beckman IR 20A instrument by using KBr pressed pellets. X-ray powder diffraction patterns were obtained with the Straumanis technique by using vanadium-filtered Cr radiation (λ_{mean} 2.2909 Å). TGA curves were obtained by using a du Pont 900 thermal analyzer coupled to a du Pont 950 thermogravimetric analyzer. Iron was determined by EDTA titrimetry. C and H analyses were performed by Integral Microanalytical Laboratories, Inc., Raleigh, N.C.

Preparation of $[Fe(Sq)(OH)(H_2O)_2]_2 \cdot 2H_2O$. Di[$\mu$-hydroxo-diaquo(squarato)iron(III)] dihydrate was prepared by adding an ethanolic solution of $FeCl_3$ to a stoichiometric amount of squaric acid dissolved in hot water. The resulting purple solution was refluxed and filtered. Upon cooling a purple-brown material crystallized. This solid was collected, repeatedly washed with cold ethanol, and air-dried at room temperature. Anal. Calcd for $FeC_4H_7O_8$: Fe, 23.38; C, 20.11; H, 2.95. Found: Fe, 23.6; C, 19.93; H, 2.84. A partially deuterated analogue was prepared by using 90% D_2O as reaction solvent. X-ray powder patterns of the normal and deuterated materials were identical.

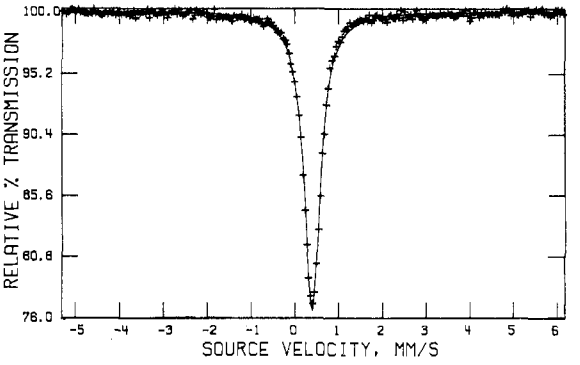

Figure 2. Room-temperature Mössbauer spectrum of $[Fe(Sq)(OH)(H_2O)_2]_2 \cdot 2H_2O$. The solid line gives the fit for a single Lorentzian line with parameters given in the text.

Results and Discussion

X-ray powder pattern d spacings obtained for the samples of $[Fe(Sq)(OH)(H_2O)_2]_2 \cdot 2H_2O$ prepared in this study are identical with those reported by West and Niu.[1] Magnetic susceptibility data for $[Fe(Sq)(OH)(H_2O)_2]_2 \cdot 2H_2O$ given in Table I[7] shown in Figure 1 indicate moderate intramolecular antiferromagnetic spin exchange in this material. Both the magnitude and temperature dependence of the susceptibility typify the behavior of an $S_1 = S_2 = {}^5/_2$ dimer.[8] For such a system the following expression for the susceptibility is obtained from the dipolar coupling approach of Van Vleck.[9]

$$\chi = (2N\beta^2g^2/kT)[(55 + 30\exp(-10J/kT) + 14\exp(-18J/kT) + 5\exp(-24J/kT) + \exp(-28J/kT))/(11 + 9\exp(-10J/kT) + 7\exp(-18J/kT) + 5\exp(-24J/kT) + 3\exp(-28J/kT) + \exp(-30J/kT))]$$

Symbols in this expression have their usual meanings. A least-squares fit of the experimental susceptibility to this equation yields values of J and g. By assuming $g = 2.00$, the smooth curves shown in Figure 1 are obtained for $J = -6.9$ cm^{-1}. This value of $|J|$ is inconsistent with both oxo- and squarato-bridged structures. Oxo-bridged Fe(III) dimers are invariably characterized by coupling constants near -100 cm^{-1}.[10] Squarate bridges, on the other hand, provide a poor exchange path as experimentally observed for the dimers $[Cu_2(Et_5dien)_2(Sq)](BPh_4)_2$ ($J = -2.1$ cm^{-1})[11] and $[Ni_2(macro)_2(Sq)](ClO_4)_2$ ($J = -0.4$ cm^{-1})[12] and for the polymeric $Ni(Sq)(H_2O)_2$ ($J = -0.7$ cm^{-1})[13] and presumably polymeric iron(II) analogue $Fe(Sq)(H_2O)_2$ ($J = -0.7$ cm^{-1}).[14] We have recently succeeded in preparing $[Fe_2(phen)_4(Sq)]Cl_4$, which we believe to contain the squarate ion bridging iron(III) ions. This complex, which provides the best model for our purposes here, has a similarily low coupling constant ($J = -0.5$ cm^{-1}).[14] Coupling constants in the range of -7 to -11 cm^{-1} have been observed for other dihydroxo-bridged Fe(III) dimers.[15,16]

A room-temperature Mössbauer spectrum of $[Fe(Sq)(OH)(H_2O)_2]_2 \cdot 2H_2O$, shown in Figure 2, may be described by a single Lorentzian line with isomer shift $\delta = 0.40$ mm/s, $\Gamma = 0.47$ mm/s. If the data are fit to a quadrupole doublet, a splitting of $\Delta = 0.16$ mm/s is obtained with $\delta = 0.40$ mm/s, $\Gamma_1 = 0.40$, and $\Gamma_2 = 0.38$ mm/s. The fit is essentially identical for these sets of parameters. Although the isomer shift increases to 0.48 mm/s at 19 K we do not observe any greater resolution of the quadrupole doublet at low temperature. These Mössbauer parameters are consistent with a near-octahedral oxygen coordination for iron(III).

Table II. Infrared Bands and Assignments (in cm^{-1})[a]

absorption	assignment
3200 br, s	ν(OH)(H_2O)
1815 sh, m	Sq, ν(C=O)
1640 sh, m	Sq, ν(C=C)
1500 br, s	Sq, ν(C–C) + ν(C–O)
1110, 1085 sh, w	Sq, ν_{13}, E_u[b]
850, 750 br, w	ν(Fe–O–H) + $\rho_r(H_2O)$
660, 460 br, w	$\rho_w(H_2O)$
420 sh, w	unassigned
390 sh, w	ν(Fe–O)
350 sh, vw	Sq, ν_2, A_{1g}[b]

[a] Abbreviations: br, broad; s, strong; sh, sharp; m, moderate; w, weak; v, very. [b] Reference 18.

Infrared spectra of squarate-containing compounds are quite characteristic of the mode of coordination.[2] Thus it is possible to distinguish the terminal form of squarate as in II from the bridging form by virtue of the lower symmetry of the former. Polymeric divalent metal squarates, which contain the squarate ion in approximately D_{4h} symmetry, have as the most prominent feature in their infrared spectra a broad band near 1500 cm^{-1} assigned to a mixture of C–O and C–C stretching modes.[1,2,12] The infrared spectrum of $[Fe(Sq)(OH)(H_2O)_2]_2 \cdot 2H_2O$, however, shows not only this absorption but also moderate bands at 1640 and 1815 cm^{-1}. The former absorption may be assigned to a C=C stretching mode and the latter to a C=O stretching mode. The infrared spectrum of this complex thus suggests nominal C_{2v} symmetry for the squarate ion, as in squaric acid and metal squarates involving bidentate coordination of the squarate ion. A number of other infrared absorptions are present in the spectrum of $[Fe(Sq)(OH)(H_2O)_2]_2 \cdot 2H_2O$, all of which are consistent with structure II.[17] These bands and appropriate assignments are listed in Table II. We have assigned a weak absorption at 850 cm^{-1} to the Fe–O–H deformation mode associated with bridging hydroxo groups.[15] This assignment is supported by the observation that this band decreases in intensity upon partial deuteration.

The thermal weight loss curve of $[Fe(Sq)(OH)(H_2O)_2]_2 \cdot 2H_2O$ obtained in a nitrogen atmosphere shows two inflections. The first, at 160 °C, corresponds to a 17.3% weight loss and the second, at 290 °C, corresponds to a 64.8% total weight loss. If the first step corresponds only to dehydration then 4.6 mol of water/mol of dimer is lost. This suggests that the hydrogen bonding between squarate and water is sufficiently strong that water coordinated to the metal, rather than water which is nominally "lattice" water, is lost first upon thermal decomposition. An X-ray powder pattern of the final residue shows the presence of iron metal. The total theoretical weight loss is 66.6% if iron metal is the only product of the decomposition. The thermal behavior of this material contrasts markedly with that of the vanadium analogue.[2] The vanadium complex loses 2 mol of water/mol of dimer at 80 °C under vacuum and 6 mol of water in either air or argon at ca. 150 °C and and, ultimately, decomposes to vanadium oxides, rather than the metal, at higher temperatures. The complexity of the final decomposition step in these complexes has been previously noted for both divalent[18,19] and trivalent[2] metal squarates.

Acknowledgment. The authors acknowledge support of this work by the Office of Naval Research.

Registry No. II, 66540-74-7.

Supplementary Material Available: A listing of observed magnetic susceptibilities, Table I (1 page). Ordering information is given on any current masthead page.

References and Notes

(1) R. West and H. Y. Niu, *J. Am. Chem. Soc.*, **85**, 2589 (1963).
(2) S. M. Condren and H. O. McDonald, *Inorg. Chem.*, **12**, 57 (1973).
(3) H. Y. Niu, Ph.D. Dissertation, University of Wisconsin, 1962.
(4) D. B. Brown, V. H. Crawford, J. W. Hall, and W. E. Hatfield, *J. Phys. Chem.*, **81**, 1303 (1977).
(5) F. E. Mabbs and D. J. Machin, "Magnetism and Transition Metal Complexes", Chapman and Hall, London, 1973, p 5.
(6) C. W. Allen and D. B. Brown, *Inorg. Chem.*, **13**, 2020 (1974).
(7) Supplementary material.
(8) S. A. Cotton, *Coord. Chem. Rev.*, **8**, 185 (1972).
(9) J. H. Van Vleck, "Electric and Magnetic Susceptibilities", Oxford University Press, London, 1932.
(10) K. S. Murray, *Coord. Chem. Rev.*, 1 (1974).
(11) Et_5dien is 1,1,4,7,7-pentaethyldiethylenetriamine. T. R. Felthouse, E. J. Laskowski, and D. N. Hendrickson, *Inorg. Chem.*, **16**, 1077 (1977).
(12) macro is 2,4,4,9,9,11-hexamethyl-1,5,8,12-tetraazacyclotetradecane. D. M. Duggan, E. K. Barefield, and D. N. Hendrickson, *Inorg. Chem.*, **12**, 985 (1973).
(13) M. Habenschuss and B. C. Gerstein, *J. Chem. Phys.*, **61**, 852 (1974).
(14) J. T. Wrobleski and D. B. Brown, to be submitted for publication.
(15) J. A. Thich, C. C. Ou, D. Powers, B. Vasiliow, D. Mastropaolo, J. A. Potenza, and H. J. Schugar, *J. Am. Chem. Soc.*, **98**, 1425 (1976).
(16) J. T. Wrobleski and G. J. Long, unpublished observations.
(17) A number of workers have discussed the infrared spectra of squaric acid, its anions, and their complexes. See for example D. P. C. Thackeray and R. Shirley, *J. Cryst. Mol. Struct.*, **2**, 159 (1972); D. P. C. Thackeray and B. C. Stace, *Spectrochim. Acta, Part A*, **30**, 1961 (1974); M. Ito and R. West, *J. Am. Chem. Soc.*, **85**, 2580 (1963); G. Doyle and R. S. Tobias, *Inorg. Chem.*, **7**, 2484 (1968).
(18) R. A. Bailey, W. N. Mills, and W. J. Tangredi, *J. Inorg. Nucl. Chem.*, **33**, 2387 (1971).
(19) C. C. Lewchalermwong, M.S. Thesis, University of North Carolina at Greensboro, 1977.

Contribution from the Department of Chemistry, University of Georgia, Athens, Georgia 30602

Poly(tertiary phosphines and arsines). 16. Some Metal Carbonyl Complexes of 1,2-Bis(dimethoxyphosphino)ethane[1]

R. B. King* and Woonza M. Rhee[2]

Received March 7, 1978

This paper presents a survey of some of the metal carbonyl chemistry of the ligand $(CH_3O)_2PCH_2CH_2P(OCH_3)_2$. This ligand is a much stronger π acceptor than the extensively studied[3] ligands $R_2PCH_2CH_2PR_2$ (R = alkyl or aryl) because of the greater electronegativity of the terminal methoxy groups. Other chelating strong π-accepting trivalent phosphorus ligands include $CH_3N(PF_2)_2$,[4-7] $F_2PCH_2CH_2PF_2$ and its homologues,[8,9,10] $(CF_3)_2PCF_2CF_2P(CF_3)_2$,[11] and $(CF_3)_2PCH_2CH_2P(CF_3)_2$.[12,13]

Experimental Section

Carbon and hydrogen analyses (Table I) were performed by the Atlantic Microanalytical Laboratory, Atlanta, Ga. Other analytical determinations (Table I) were performed by Schwarzkopf Microanalytical Laboratory, Woodside, N.Y. Melting and decomposition points (Table I) were taken in capillaries and are uncorrected.

Infrared spectra in the ν(CO) region (Table I) were taken in pentane, hexane, or dichloromethane solutions and recorded on a Perkin-Elmer Model 621 spectrometer with grating optics. Each spectrum was calibrated against the 1601-cm^{-1} band of polystyrene film. Proton NMR spectra (Table I) were taken in $CDCl_3$ solutions and recorded on a Varian T-60 spectrometer at 60 MHz.

All solvents including triethylamine used in reactions were freshly distilled under nitrogen from appropriate drying agents (Na/$(C_6H_5)_2CO$, $LiAlH_4$, etc.). All reactions were run under nitrogen. The air-sensitive $(CH_3O)_2PCH_2CH_2P(OCH_3)_2$ was handled in a nitrogen-filled glovebox (Vacuum Atmospheres).

The $Cl_2PCH_2CH_2PCl_2$ was obtained from white phosphorus, phosphorus trichloride, and ethylene according to the patented procedure.[14]

Preparation of $(CH_3O)_2PCH_2CH_2P(OCH_3)_2$ (abbreviated as Pom-Pom). A mixture of 16.7 mL (12.1 g, 120 mmol) of tri-

0020-1669/78/1317-2961$01.00/0